

# Up-regulation of matrix metalloproteinase-3 in the dorsal root ganglion of rats with paclitaxel-induced neuropathy

Kentaro Nishida,<sup>1</sup> Satoshi Kuchiiwa,<sup>2</sup> Shigeru Oiso,<sup>1</sup> Toshitaka Futagawa,<sup>1</sup> Shogo Masuda,<sup>1</sup> Yasuo Takeda<sup>1,3</sup> and Katsushi Yamada<sup>1</sup>

<sup>1</sup>Department of Clinical Pharmacy and Pharmacology, <sup>2</sup>Department of Neuroanatomy, Graduate School of Medical and Dental Sciences, Kagoshima University, 8-35-1 Sakuragaoka, Kagoshima 890-8520, Japan

(Received February 27, 2008/Revised April 12, 2008/Accepted April 25, 2008/Online publication July 29, 2008)

Paclitaxel-induced painful peripheral neuropathy is a major dose-limiting factor. Recently, it has been reported that macrophages accumulated in the dorsal root ganglion of paclitaxel-treated rats, and their activation is suggested to contribute to generation and development of the neuropathy. However, the mechanism for macrophage activation is still unknown. In this study, to explore candidate genes involved in the mechanism for macrophage activation in the dorsal root ganglion of paclitaxel-treated rats, we developed model rats for paclitaxel-induced neuropathic pain and performed a microarray assay to analyze the changes of gene expressions in the dorsal root ganglion. Among the genes with changed expression levels, we focused on *matrix metalloproteinase-3 (MMP-3, stromelysin-1)* and *CD163*, a macrophage marker. By reverse transcription-polymerase chain reaction, the expression levels of MMP-3 and CD163 were markedly up-regulated in paclitaxel-treated dorsal root ganglion. As a result of immunohistochemical study, large ganglion neurons, but neither Schwann cells nor macrophages, predominantly expressed MMP-3. This MMP-3 up-regulation occurred prior to macrophage accumulation in the dorsal root ganglion. In addition, recombinant MMP-3 led to the activation of RAW264 macrophages *in vitro*. Taken together, the up-regulation of MMP-3 and following macrophage activation caused in the dorsal root ganglion might be a significant event to trigger a series of reactions developing paclitaxel-induced peripheral neuropathic pain. (*Cancer Sci* 2008; 99: 1618–1625)

Paclitaxel is an antineoplastic agent used clinically to treat non-small-cell lung cancer and ovarian cancer.<sup>(1,2)</sup> Paclitaxel suppresses microtubule dynamics, causing mitotic arrest in dividing cells.<sup>(3)</sup> On the other hand, painful peripheral neuropathy is a major dose-limiting factor in clinical cancer chemotherapy with paclitaxel.<sup>(4,5)</sup> Although the administration of glutamine and acetyl-L-carnitine has been reported to relieve paclitaxel-induced neuropathic pain as symptomatic treatment,<sup>(6,7)</sup> its effectiveness shows large interindividual variation. To develop a specific treatment, the molecular mechanisms underlying paclitaxel-induced neuropathy should be explored.

It has been assumed that paclitaxel-induced neuropathy is generally due to effects on axonal microtubules.<sup>(8)</sup> Paclitaxel-induced neuropathy is characterized by an ascending distal paresthesia and dysesthesia in a 'glove and stocking' distribution.<sup>(5,8)</sup> Blocking of axonal transport due to paclitaxel-induced disruption of microtubule dynamics, which seems to be a reasonable mechanism, has been observed *in vitro*.<sup>(9)</sup> Nerve biopsies from patients with taxane-induced neuropathy have shown evidence of a loss of large diameter afferents.<sup>(10)</sup> In contrast, it has been reported that administration of low dose of paclitaxel caused neuropathic pain without any change of axonal morphology.<sup>(11)</sup> Additively, *in vitro*, axonal transport was not impaired in DRG

neurons exposed to paclitaxel at chemotherapeutic doses.<sup>(12)</sup> Thus, it is reasonable to suspect that paclitaxel-induced neuropathy is due to beta-tubulin binding and subsequent disruption of microtubular axoplasmic flow. Further evidence to support this hypothesis is still necessary.

Recently, some animal models for neuropathy have been developed,<sup>(11,13)</sup> and valuable information to understand the events occurring in the DRG has been obtained from these models. Among them, Matsumoto *et al.* demonstrated that the expression levels of mRNA and protein of calcium channel subunit  $\alpha 2\delta$ -1, one of the putative targets for gabapentin, are significantly increased in the DRG after paclitaxel treatment.<sup>(14)</sup> In addition, some studies have reported marked change in the expressions of vanilloid receptor 1,  $\mu$ -opioid receptor, and adrenoreceptor  $\alpha 2A$  in the DRG after nerve injury.<sup>(15–17)</sup> The alteration of gene and protein expressions in the DRG observed in neuropathic pain models and nerve injury has been suggested to contribute to the generation and development of neuropathic pain. Recently, Peter *et al.* reported that macrophages accumulated in the DRG of paclitaxel-treated rats, and this cellular pathology was accompanied by behavioral changes,<sup>(18)</sup> but the mechanism underlying macrophage accumulation/activation is still unknown. Collectively, it is reasonable to speculate that potential molecule(s) which induce macrophage accumulation and/or activation in the DRG of paclitaxel-treated rats might play a key role in the development of neuropathic pain.

Therefore, the purpose of the present study was to explore candidate genes involved in macrophage activation in the DRG of paclitaxel-treated rats with a cDNA microarray, and among neuropathic pain-related genes, we focused on *MMP-3* (stromelysin-1), and its alteration was investigated in more detail.

## Materials and Methods

**Animals and study design.** Male Sprague–Dawley rats (340–390 g; Japan SLC, Japan) were used in these experiments. The study was approved by the Graduate School of Medical and Dental Sciences of Kagoshima University and was conducted in accordance with the Guidelines for Animal Experimentation by

<sup>3</sup>To whom correspondence should be addressed.

E-mail: takeda@m.kufm.kagoshima-u.ac.jp

Abbreviations: ATF3, activation transcription factor-3; DMEM, Dulbecco's modified Eagle's medium; DRG, dorsal root ganglion; GAPDH, glyceraldehyde 3-phosphate dehydrogenase; HBSS, Hanks' balanced salt solution; HRP, horseradish peroxidase; LDH, lactic dehydrogenase; MMP-3, matrix metalloproteinase-3; NNGH, N-isobutyl-N-(4-methoxyphenylsulfonyl)glycyl hydroxamic acid; MTT, 3-[4,5-dimethyl-2-thiazolyl]-2,5-diphenyl-2H-tetrazolium bromide; PAP, peroxidase-antiperoxidase; PBS, phosphate-buffered saline; ROS, reactive oxygen species; RT-PCR, reverse transcription-polymerase chain reaction.

the International Association for the Study of Pain.<sup>(19)</sup> Paclitaxel (Taxol; generously provided by Bristol-Myers-Squibb, Paris, France) was injected intraperitoneally (i.p.) at a dose of 16 mg/kg once a day on day 1 and 3, the cumulative dose being 32 mg/kg, and the control rats were administered the same volume of a vehicle solution (Cremophor EL/ethanol, 1:1 [v/v]).

**Behavioral analysis.** Behavioral evaluation of mechanical hyperalgesia of the hind paw was tested using a dynamic plantar aesthesiometer (Ugo Basile, Italy), following the manufacturer's instructions. Briefly, as for mechanical hyperalgesia, plantar von Frey hairs were used to detect changes in touch sensitivity in response to mechanical stimulation (force increasing rate: 2.5 g/s, cut-off time: 20 s), resulting from neural damage. Each left and right hind paw was tested three times or more with a 3-min interval between trials, and all evaluations were performed under blind conditions.

**Antibodies.** The antibodies used for analyses were as follows: rabbit antiactivation transcription factor-3 (ATF3) antibody (1:300; Santa Cruz Biotechnology, Santa Cruz, CA, USA), goat antirabbit IgG antibody (1:2000; EY Laboratories, CA, USA), PAP complex solution (1:1000; Dako, Denmark), mouse monoclonal anti-MMP-3 antibody (clone 55-2A4, 1:300; Daiichi Fine Chemicals, Japan), mouse monoclonal anti-GAPDH antibody (clone 6C5, 1:50 000; Applied Biosystems, CA, USA), rabbit anti-S100 antibody (1:200, Sigma, USA), rabbit anti-Iba1 antibody (1:100, Wako, Japan), goat antimouse rhodamine and antirabbit FITC antibodies (1:500; Cappel, OH, USA), and HRP-conjugated goat antimouse and rabbit antibodies (1:1000, Nacalai Tesque, Japan).

**Immunohistochemical analyses.** The immunohistochemical detection of ATF3 was performed with the PAP method.<sup>(20)</sup> The animals were perfused transcardially with 4% paraformaldehyde in 0.1 M phosphate buffer (pH 7.4) containing 0.2% picric acid under deep anesthesia (pentobarbital sodium, 40 mg/kg, i.p.). DRGs isolated from lumbar 4 and 5 levels were sectioned at 40  $\mu$ m thickness with a freezing microtome, and serial longitudinal sections were treated with 0.3% hydrogen peroxide in 0.02 M PBS for 15 min at room temperature. Then the sections were incubated for 3 days at 4°C in rabbit anti-ATF3 in PBS with 1% normal goat serum and 0.3% Triton-X-100, followed by incubation for a day at 4°C with goat antirabbit IgG antibody and antirabbit PAP complex solution. Thereafter the sections reacted with 0.02% 3,3'-diaminobenzidine tetrahydrochloride (Dojindo, Japan), 0.003% hydrogen peroxide, and 0.43% ammonium nickel sulfate. The sections were mounted on glass slides. Immunohistochemical observation was performed using light microscopy (Keyence, Japan).

For fluorescent immunohistochemistry, free-floating sections were immunoreacted with primary antibodies, mouse anti-MMP-3, rabbit anti-S100, and rabbit anti-Iba1 antibodies in PBS with 1% normal goat serum and 0.3% Triton-X-100 for 3 days at 4°C, and then incubated with a mixture of two secondary antibodies, goat antimouse IgG conjugated rhodamine, and goat antirabbit IgG conjugated FITC, in PBS for a day. The sections were mounted on glass slides. Images were acquired using a confocal laser-scanning microscope (Leica, Germany).

**Microarray analysis.** The patterns of various mRNAs expressions in DRGs were analyzed by the GeneChip array provided by Kurabo custom analysis services (Japan). Briefly, we used a GeneChip Rat Genome 230 2.0 array (Affymetrix) according to the manufacturer's protocol. Raw intensity data from the array were analyzed by GeneChip Operating Software (Affymetrix). According to the manufacturer's instructions, gene expressions changing more than two-fold in a signal log ratio between target and control groups were significantly different, and either up- or down-regulated.

**Semiquantitative RT-PCR.** One microgram of total RNAs extracted from control or paclitaxel-treated DRGs were reverse transcribed to cDNA by using SuperScript II Reverse Transcriptase (Invitrogen,

USA). PCR products were analyzed on 1% agarose gel. For standardization, rat GAPDH was used. The primers for detection of MMP-3, CD163, and arginase-1 cDNAs were as follows: MMP-3, 5'-GATGGTATTCAATCCCTCTATGGACC-3' (forward) and 5'-CCGCTGAAGAAGTAAAGAAACC-3' (reverse); CD163, 5'-GATCTGGCATAGAGGTTCT-3' (forward) and 5'-TCAGCA-AGTCCAGATCATCC-3' (reverse); arginase-1, 5'-AAAGCCCAT-AGAGATTATCGGAGCG-3' (forward) and 5'-AGACAAG-GTCAACGGCACTGCC-3' (reverse).<sup>(21)</sup> MMP-3 and CD163 cDNAs were amplified for 35 cycles at 94°C for 15 s, 55°C for 30 s, and 68°C for 30 s; and arginase-1 amplified were for 33 cycles at 94°C for 15 s, 67°C for 30 s, and 68°C for 60 s. The PCR for GAPDH was carried out using the primers 5'-CGTCTTACCATTGGAGA-3' (forward) and 5'-CGGCCAT-ACGCCACAGTTT-3' (reverse) at 94°C for 30 s, 55°C for 30 s, and 72°C for 30 s for 28 cycles. The sequences of PCR products were matched with those of rat MMP-3 (NM\_133523) and CD163 (NM\_001107887).

**Western blot analyses.** Western blot analyses were performed using specific antibodies for MMP-3 and GAPDH. Signals reacting with primary antibodies were detected using HRP-linked secondary antibodies and enhanced by a chemiluminescence detection system (GE Healthcare, UK). Protein concentrations were determined using the Lowry method.<sup>(22)</sup>

**Recombinant MMP-3 pretreatment.** Recombinant proenzyme MMP-3 (Merck, Germany) was activated by incubation in 50 mM Tris, pH 7.5, containing 0.05% Triton-X-100, 5 mM CaCl<sub>2</sub>, and 1 mM 4-aminophenylmercuric acetate for 4 h at 37°C.

**Cell culture and ROS measurement.** The RAW264 murine macrophage cell line was obtained from the Riken Bioresource Center (Japan). Cells were maintained in Dulbecco's modified Eagle's medium (DMEM) (Gibco, USA) supplemented with 10% FBS, 100-U/mL penicillin, and 0.1 mg/mL streptomycin in a humidified atmosphere of normal culture condition. RAW264 were treated with recombinant MMP-3 (active form) and/or NNGH (Biomol, USA), N-acetyl-L-cysteine (NAC; Wako, Japan), or EUK-8 (Calbiochem, Darmstadt, Germany) in hydroxyphenyl fluorescein (HPF; Daiichi Pure Chemical, Japan) mixed with HBSS (Nissui, Japan) for 1 h. Then the fluorescence signals were detected using laser confocal microscopy (FV500; Olympus, Tokyo, Japan).

**Cell viability determination.** After 1-h treatment of RAW264 cells with recombinant MMP-3, the cells were incubated in fresh DMEM containing 0.5 mg/mL MTT (Dojindo, Kumamoto, Japan) for 4 h. Thereafter, 20% sodium dodecyl sulfate solution was added to extract MTT formazan, and then the absorbance at 570 nm was measured using a microplate reader. We confirmed that the decrease in cell viability observed in the MTT assay was not caused by mitochondrial dysfunction, by comparison with the results obtained on LDH assay.

**Statistical analyses.** Data were presented as the mean  $\pm$  standard error or SD. Comparisons of data between the control and paclitaxel-treated groups were analyzed using the Student's *t*-test. *P* < 0.05 was considered significant.

## Results

**Paclitaxel induced mechanical hyperalgesia in rats.** First, we evaluated the validity of our rat model to investigate the molecular mechanisms underlying paclitaxel-induced neuropathy. On day 1, there were no differences in the hind paw mechanical withdrawal thresholds between control and paclitaxel-treated rats. In contrast, on day 10, the threshold of paclitaxel-treated rats was significantly less than that of control rats (Fig. 1a), indicating the induction of mechanical hypersensitivity, that is, mechanical hyperalgesia caused by paclitaxel treatment.

**ATF3 immunoreactivity in the lumbar DRG of paclitaxel-treated rats.** To confirm the involvement of nerve injury in paclitaxel-induced

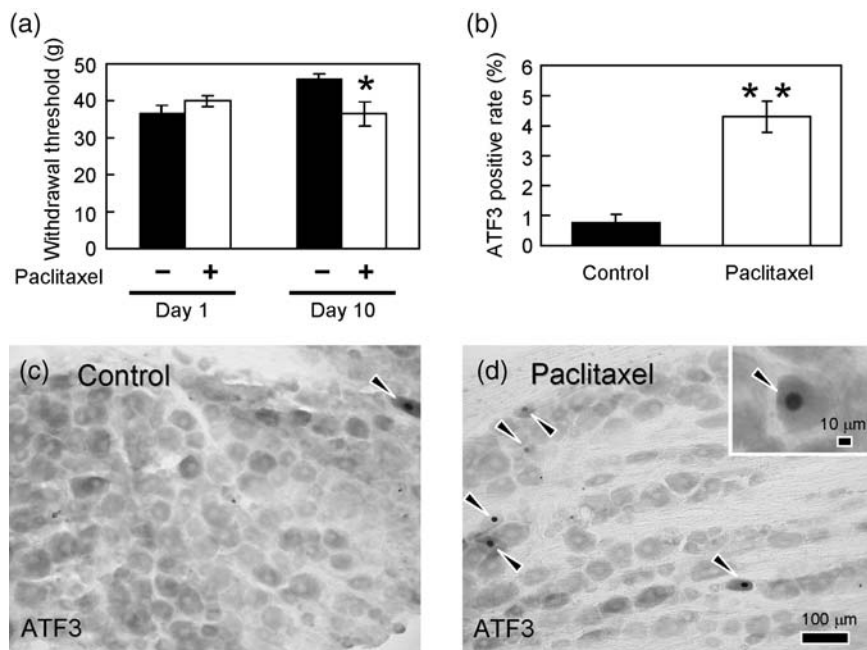


**Fig. 1.** Paclitaxel-induced mechanical hyperalgesia in rats and expression of activation transcription factor-3 (ATF3) in lumbar dorsal root ganglions (DRGs). (a) Behavioral analysis was performed with a dynamic plantar aesthesiometer on day 1 and 10. Data show the mean  $\pm$  SE ( $n = 5$ ) \* $P < 0.05$ , versus control. (b) On day 10 following the dosing schedule of paclitaxel, isolated lumbar DRGs were sectioned and immunostained with the specific antibody against ATF3. Panel (b) shows the quantitative results of ATF3-positive nuclei. Each column represents the mean  $\pm$  SE ( $n = 6-7$ ) \*\* $P < 0.01$ , versus control. (c, d) Microphotographs show representative immunostaining of ATF3 in the nuclei of DRG of either control (c) or paclitaxel-treated rats (d). Arrowheads indicate ATF3-positive nuclei.

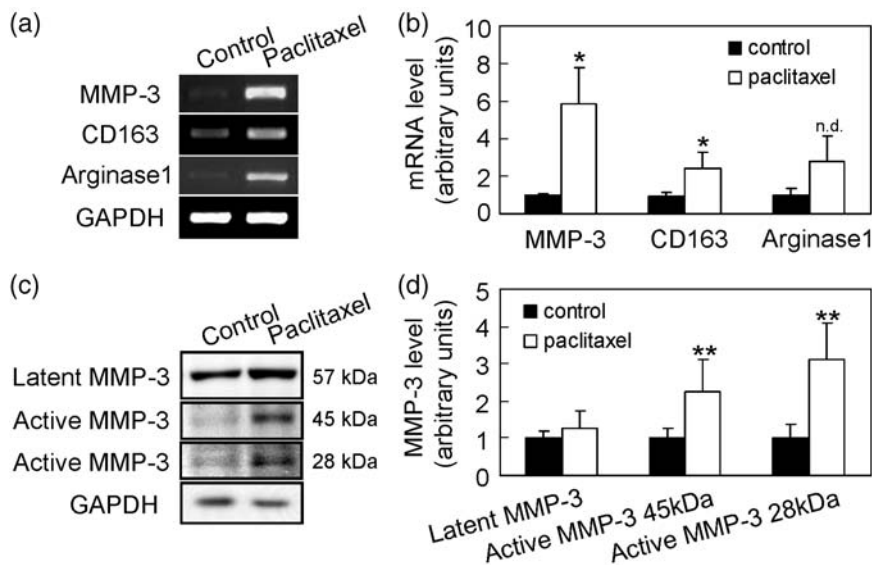


**Fig. 2.** Expression of matrix metalloproteinase-3 (MMP-3), CD163, and arginase-1 in the lumbar dorsal root ganglion (DRG) of paclitaxel-treated rats. On day 10 following the dosing schedule of paclitaxel, total RNA was extracted from lumbar DRGs, and the expressions of MMP-3, CD163, and arginase-1 were determined by semiquantitative reverse transcription-polymerase chain reaction (a,b). Panel (b) shows the quantitative results after correction by the corresponding glyceraldehyde 3-phosphate dehydrogenase (GAPDH) mRNA expression shown in panel (a). Each column represents the mean  $\pm$  SD ( $n = 3$ ). \* $P < 0.05$ , versus control. In panel (c), latent and active forms of MMP-3 were detected as bands of 57, 45, and 28 kDa, respectively. Panel (d) shows the quantitative results after correction by the corresponding GAPDH protein expression shown in panel (c). Each column represents the mean  $\pm$  SD ( $n = 6$ ). \*\* $P < 0.01$ , versus control.

mechanical hyperalgesia, the expression of ATF3, a marker of nerve injury,<sup>(23)</sup> in the DRG was examined. A signal related to ATF3 in the DRG of control rats was hardly detectable, while apparent ATF3 immunoreactivity was observed in neuronal nuclei in the lumbar DRG of paclitaxel-treated rats (Fig. 1c,d). The percentage of ATF3-positive nuclei in the DRG of paclitaxel-treated rats ( $4.31 \pm 0.52\%$ ,  $n = 6$ ) was significantly greater than that in control rats ( $0.77 \pm 0.25\%$ ,  $n = 7$ ; Fig. 1b). Taken together with the aforementioned hyperalgesia, paclitaxel-induced neuropathic pain was demonstrated to be caused by neuronal injury in the DRG at day 10.

**Microarray analysis on the lumbar DRG of paclitaxel-treated rats.**

To find candidate genes involved in macrophage activation in the DRG of paclitaxel-treated rats, we performed the microarray assay to analyze changes of gene expression in the lumbar DRG of paclitaxel-treated rats. On day 10 following to the dosing schedule of paclitaxel, 0.19% (60 of 31 099) of genes were significantly up-regulated in paclitaxel-treated rats compared to the controls (Table 1). On the other hand, 0.12% (38 of 31 099) of

genes were significantly down-regulated (Table 2). Furthermore, we performed a gene ontology analysis to classify the genes into several categories. Interestingly, 26 of 60 up-regulated genes (43%) were involved in the inflammatory and/or immune responses (indicated by asterisks in Table 1). Among these, we focused on the CD163, which is dominantly expressed in macrophages, and MMP-3. It was because paclitaxel treatment induced macrophages to activate and/or accumulate in the DRG,<sup>(18,24,25)</sup> and administration of recombinant MMP-3 increased to produce ROS in the microglial cells.<sup>(26)</sup> The expression levels of MMP-3 and CD163 mRNAs in the DRGs were markedly increased in paclitaxel-treated rats (Fig. 2a,b), while arginase-1, a marker for macrophage activation,<sup>(21)</sup> showed a tendency to increase in its expression level in the paclitaxel-treated DRGs. These results suggest that paclitaxel apparently induced up-regulation of MMP-3 and accumulation/activation of macrophages in the DRGs.

MMP-3 has three different forms of which one is latent (57 kDa) and the other two are active (28 and 45 kDa). We next determined whether active forms of MMP-3 were up-regulated

**Table 1. Increased gene expression in the lumbar dorsal root ganglion (DRG) of paclitaxel-treated rats**

Gene name	Accession number	Signal log ratio
Phospholipase-A2, group IIA (platelets, synovial fluid)*	NM_031598	6.9
RT1 class Ib, locus Aw2	NM_001008829	6.0
Chemokine (C-C motif) ligand 21b (serine)*	NM_001008513	5.5
Butyrophilin-like-8*	NM_212489	4.9
Potassium inwardly rectifying channel, subfamily J, member-16	NM_053314	4.3
Myotubularin-related protein-1 (predicted)	XM_228644	4.1
Similar to small inducible cytokine B13 precursor (CXCL13)*	NM_001017496	3.9
Chemokine (C-X-C motif) ligand-1*	NM_030845	3.6
Phospholipase-A2, group IID	NM_001013428	3.6
Lipopolysaccharide binding protein*	NM_017208	3.5
Fc gamma receptor-II-beta*	XM_573502	3.3
Fc receptor, IgG, low affinity IIb*	NM_175756	3.3
Chitinase 3-like-1	NM_053560	3.3
Coagulation factor C homolog ( <i>Limulus polyphemus</i> ) (predicted)	XM_343058	3.3
Similar to suprabasal-specific protein suprabasin (predicted)	XM_214902	3.3
Glycoprotein-49b*	NM_001013894	3.2
Complement component-1, q subcomponent, gamma polypeptide*	NM_001008524	3.1
Complement factor-B*	NM_212466	3.1
Fc receptor, IgG, low affinity III*	NM_053843	3.0
Ceruloplasmin	NM_012532	3.0
Mast cell protease-1	NM_017145	2.9
Complement component-3*	NM_016994	2.8
Gap junction membrane channel protein-beta-6	NM_053388	2.8
CD163 antigen (predicted)*	XM_232342	2.7
Complement component-1, q subcomponent, alpha polypeptide*	NM_001008515	2.7
Complement component-1, q subcomponent, beta polypeptide*	NM_019262	2.7
Keratin complex-1, acidic, gene 19	NM_199498	2.7
Serine (or cysteine) peptidase inhibitor, clade A, member 3 N	NM_031531	2.7
Amyloid beta (A4) precursor protein-binding, family B, member-1 interacting protein	XM_225631	2.6
Epoxide hydrolase-2, cytoplasmic*	NM_022936	2.6
Insulin-like growth factor binding protein-6	NM_013104	2.6
Similar to scavenger receptor type A SR-A (predicted)	XM_573919	2.6
X transporter protein-3	NM_133296	2.5
Macrophage galactose N-acetyl-galactosamine specific lectin-1*	NM_022393	2.4
Glycoprotein (transmembrane) nmb, osteoactivin	NM_133298	2.4
Selectin, platelet*	NM_013114	2.3
Similar to BAZF (predicted)	XM_340830	2.3
CD14 antigen*	NM_021744	2.2
Complement component-4a*	NM_001002805	2.2
Gap junction membrane channel protein-beta-2	NM_001004099	2.2
Membrane-spanning 4-domains, subfamily A, member-11 (predicted)	XM_342028	2.2
Similar to hypothetical protein FLJ21986	XM_575402	2.2
Chemokine (C-X-C motif) ligand-14*	NM_001013137	2.1
Complement component-1, s-subcomponent*	NM_138900	2.1
Alpha-2μ globulin PGCL4	NM_001033958	2.1
Coagulation factor XIII, A1 subunit	NM_021698	2.1
Matrix metalloproteinase-3*	NM_133523	2.1
Stimulated by retinoic acid gene 6 homolog (mouse)	NM_001029924	2.1
Ubiquitin carboxyl-terminal hydrolase L5	NM_001012149	2.1
Cathepsin-S*	NM_017320	2.0
Complement factor-D (adipsin)*	XM_343169	2.0
CCAAT/enhancer binding protein (C/EBP), delta	NM_013154	2.0
Chondroitin sulfate proteoglycan-2	XM_215451	2.0
Dendritic cell inhibitory receptor-3	NM_001005891	2.0
Epithelial membrane protein-1	NM_012843	2.0
Epithelial V-like antigen-1 (predicted)	XM_236197	2.0
Insulin responsive sequence DNA binding protein-1	XM_237415	2.0
Mannose receptor, C type 1 (predicted) CD206	XM_225585	2.0
Nuclear protein-1	NM_053611	2.0
Osteoglycin (predicted)	NM_001106103	2.0

Asterisks indicate increased gene expression of inflammatory and/or immune response-related genes.

**Table 2. Decreased gene expression in the lumbar dorsal root ganglion (DRG) of paclitaxel-treated rats**

Gene name
Hemoglobin-beta chain complex
Hemoglobin-alpha, adult chain-1
Globin-alpha
Bone gamma-carboxyglutamate protein-2
Cathelicidin antimicrobial peptide
CD79B antigen
Similar to spermatogenesis-associated glutamate (E)-rich protein-4d
Membrane-spanning 4-domains, subfamily A, member-1 (predicted)
RT1 class Ib, locus Aw2
Nuclear receptor corepressor-1
ATPase, Ca + + transporting, cardiac muscle, fast twitch-1
Prostaglandin-F receptor
Cytochrome-P450, family 2, subfamily A, polypeptide-3a
Matrix metalloproteinase-9
Solute carrier family 24 (sodium/potassium/calcium exchanger), member-2
Ig active lambda2-like chain mRNA, 3' end
Procollagen, type II, alpha-1
S100 calcium binding protein A9 (calgranulin B)
Similar to Myosin IXb (Unconventional myosin-9b)
Dentin matrix protein-1
Erythroid associated factor (predicted)
Integrin binding sialoprotein
Solute carrier family 4, member-1
SNF1-like kinase
S100 calcium binding protein A8 (calgranulin A)
Similar to immunoglobulin heavy chain-6 (Igh-6)
LOC501485
XK-related protein-4
Myosin, light polypeptide-2
Mast cell protease-8
Procollagen, type IX, alpha-1
Acid phosphatase-5, tartrate resistant
Aminolevulinic acid synthase-2
Myosin, heavy polypeptide-4, skeletal muscle
Phosphatidylinositol-3-kinase, C2-domain-containing, gamma polypeptide
Fast myosin alkali light chain
Leukocyte cell-derived chemotaxin-1
Similar to IG kappa chain V-V region K2 precursor

by paclitaxel treatment. Western blot analysis showed that the expression levels of active forms (28 and 45 kDa) of MMP-3 were significantly increased in the DRGs of paclitaxel-treated rats, while the latent form (57 kDa) was steady (Fig. 2c,d). It is known that mast cell protease 1 is one of processing enzymes to cleave MMP-3 to its active forms.<sup>(27)</sup> According to our microarray analysis, mRNA expression levels of mast cell protease 1 in the DRGs was greatly up-regulated by paclitaxel treatment (Table 1), suggesting that the acceleration of MMP-3 cleavage consequently kept the latent form steady.

**MMP-3 immunoreactivity in the lumbar DRG of paclitaxel-treated rats.** To identify which type of cells in DRGs express the MMP-3 by paclitaxel treatment, we next examined the localization of MMP-3-like immunoreactivity in the lumbar DRGs. There was no detectable signal in the control rat preparations stained with anti-MMP-3 antibody (Fig. 3a), while many immunoreactive large cell bodies were observed in the lumbar DRGs of the rats on day 10 following the dosing schedule of paclitaxel (Fig. 3b, arrowheads). In the paclitaxel-treated rats, the MMP-3 like immunoreactivity was located in the perikarya but neither in the nuclei nor axons.

The immunopositive cells of the S100, the marker of the large neurons, Schwann cells and satellite cells,<sup>(28)</sup> were distributed in the DRG of the rats on day 10 following the dosing schedule of paclitaxel. The S100-like immunoreactive fluorescent labeled substances were found mainly in the large neuronal cell bodies and the axons derived from the large neurons (Fig. 3d, asterisks), and furthermore, fewer small cells were found in close to the fiber bundles, they were spindle in shape and regarded as the Schwann cells (Fig. 3d, arrows). The other type of labeled small cells were also found around the large ganglion neurons, regarded the satellite cells (Fig. 3d, arrowheads). In the double-stained fluorescent immunohistochemical preparations, the MMP-3-like immunoreactive substances and the S100-like immunoreactive granules coexisted in a part of the large neuronal cell bodies (Fig. 3e, asterisks), but neither in the small ganglion neurons, Schwann cells, or satellite cells (Fig. 3e, arrows and arrowheads).

In the immunostaining preparations of MMP-3 and Iba1, a macrophage marker,<sup>(29)</sup> MMP-3-positive cells in the control rats were not detectable, but on days 6, 8, and 10, MMP-3-like immunoreactivity was markedly up-regulated and dominantly detected in a part of the large ganglion neurons (Fig. 4a1-d1, arrowheads). Namely, the MMP-3-like immunoreactivity was expressed on day 6 after paclitaxel treatment (Fig. 4b1, arrowheads). On the other hand, Iba1-like immunoreactivity was observed in small cells in the control and paclitaxel treated preparations (Fig. 4a2-d2). The density of Iba1-like immunoreactive cells was relatively low in the control preparation, and the cell density was not increased on day 6 after paclitaxel treatment (Fig. 4a2,b2). However, on days 8 and 10, the Iba1-like immunoreactive small cells were greatly increased in density (Fig. 4c2,d2). Namely, Iba1-like immunoreactivity expression in the macrophages occurred about 2 days later than MMP-3-like immunoreactivity expression in the large neurons did. On the other hand, at any time-points there was no colocalization of MMP-3-like and Iba1-like immunoreactivity (Fig. 4b3-d3).

**Recombinant MMP-3 activates macrophages.** To confirm that MMP-3 activates macrophages, we examined the generation of ROS in macrophages treated by MMP-3 *in vitro*. After treatment with recombinant MMP-3 for 1 h, ROS expression was strongly up-regulated in RAW264 macrophages in a concentration-dependent manner (0–12.5 ng/mL MMP-3), except when treated with a higher concentration of MMP-3. Because of this, the lower signal in 125–250 ng/mL may be due to strong cytotoxicity affected by the large amount of ROS generated by MMP-3 (Fig. 5a,c).

We next examined the effect of MMP-3 inhibitor on ROS generation. NNGH, an MMP-3 inhibitor, perfectly blocked MMP-3-induced ROS generation (Fig. 5b). Besides NNGH, antioxidants NAC and EUK-8 also strongly blocked it as well (Fig. 5b). Furthermore, NAC dose-dependently recovered MMP-3-induced cytotoxicity possibly via its scavenging effect on ROS (Fig. 5c). These findings indicate that MMP-3 directly activates macrophages and induces up-regulation of ROS, cytotoxic factor.

## Discussion

The purpose of this study was to explore candidate genes which can activate macrophages as potential targets for the treatment of paclitaxel-induced neuropathy. In this study, paclitaxel caused mechanical hyperalgesia (Fig. 1a). Authier *et al.*<sup>(13)</sup> reported that paclitaxel single administration at a dose of 32 mg/kg induced hind paw mechanical hyperalgesia, this dose being the same with our cumulative dose of 32 mg/kg. In addition to mechanical hyperalgesia, rats treated with paclitaxel, as well as cancer patients,<sup>(4)</sup> were reported to develop thermal hyperalgesia.<sup>(11,18)</sup> We also examined withdrawal frequency against acetone and a hot plate on day 10 (data not shown). Our model rats for paclitaxel-induced neuropathy developed cold allodynia, but not heat hyperalgesia, consistent with the model rats reported

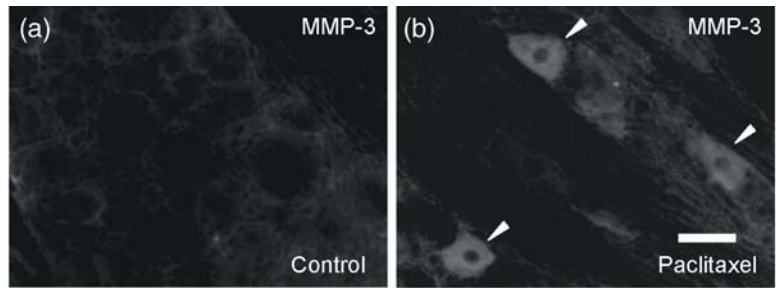


**Fig. 3.** Matrix metalloproteinase-3 (MMP-3) immunoreactivity in lumbar dorsal root ganglions (DRGs). On day 10 following the dosing schedule of paclitaxel, longitudinal sections of lumbar DRGs were fluorescently immunostained with anti-MMP-3 antibody (a,b) and double-immunostained in combination with antibodies against MMP-3 and S100 (c–e). Arrowheads indicate MMP-3-positive cells (b). S100 immunoreactivity was detected in round neurons (asterisks, c and e), in spindly Schwann cells (arrows, d and e), and in satellite cells (arrowheads, d and e). Scale bar is 50  $\mu\text{m}$ .

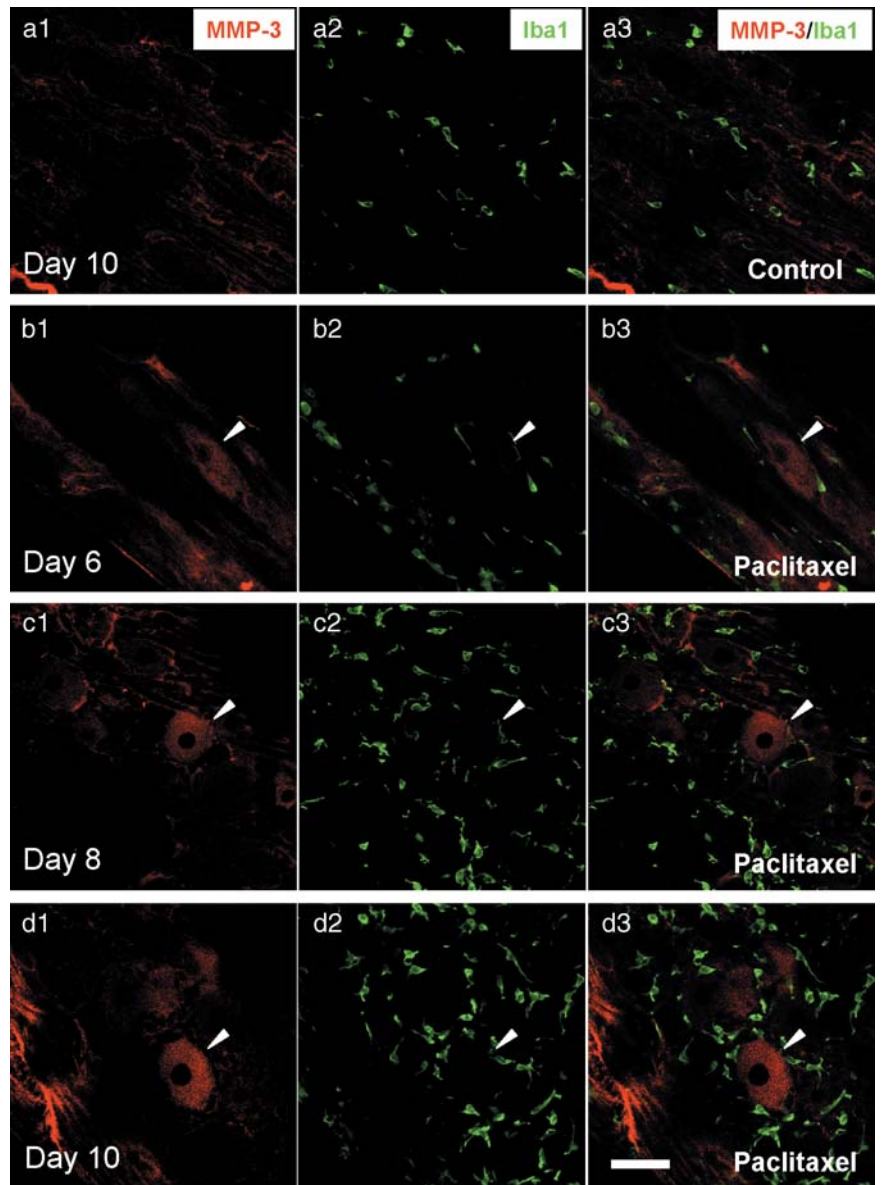
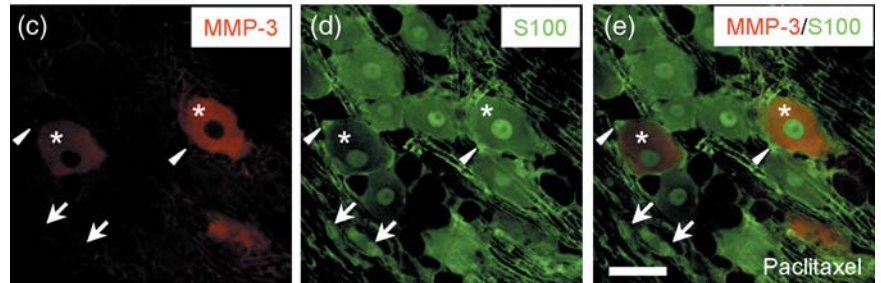


**Fig. 4.** Accumulation and localization of macrophages in lumbar dorsal root ganglions (DRGs). On day 6, 8, and 10 following the dosing schedule of paclitaxel, longitudinal sections of lumbar DRGs were fluorescently double-immunostained in combination with antibodies against matrix metalloproteinase-3 (MMP-3) and Iba1, a macrophage marker. Left and middle panels represent representative immunostaining for MMP-3 (a1, b1, c1, and d1) and Iba1 (a2, b2, c2 and d2), respectively, and right panels show their merged microphotographs (a3, b3, c3, and d3) for at least three independent experiments. MMP-3 immunoreactivity was detected in large ganglion neurons (arrowheads). Scale bar is 50  $\mu\text{m}$ .

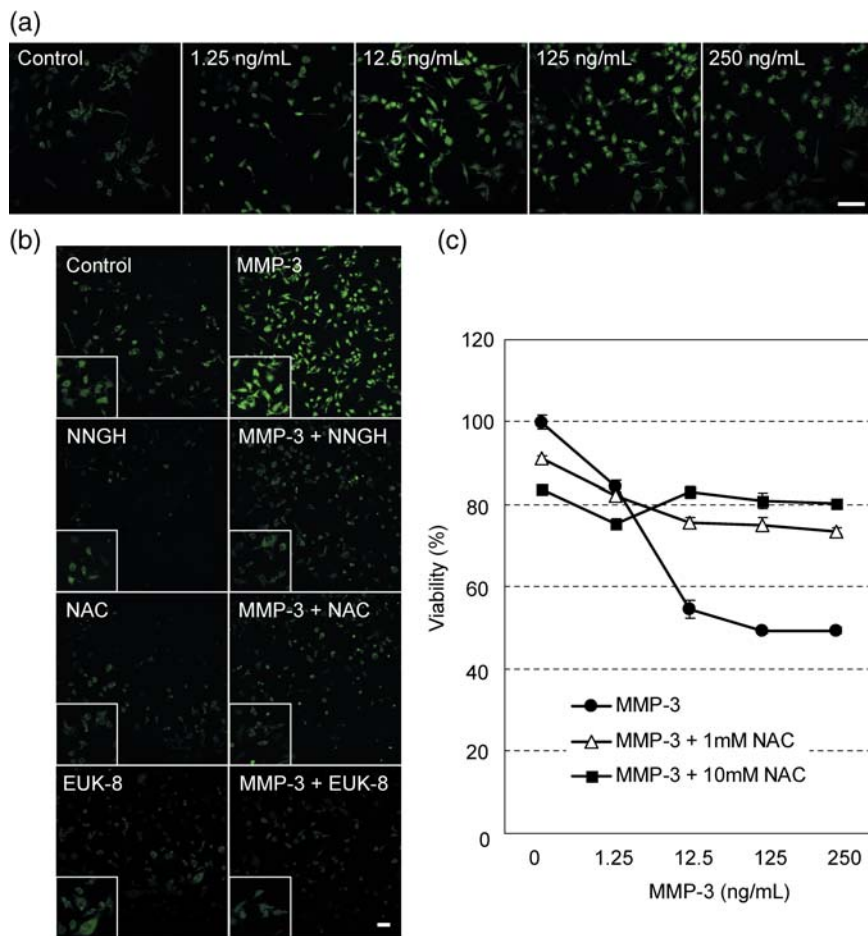


**Fig. 5.** Effect of recombinant matrix metalloproteinase-3 (MMP-3) on reactive oxygen species (ROS) generation and cell viability in macrophage-like cells. After RAW264 cells were incubated in horseradish peroxidase containing Hank's balanced salt solution (HBSS) for 15 min, they were exposed to the indicated concentrations of recombinant MMP-3 in the same media for 1 h. To inhibit MMP-3 enzymatic activity and scavenge generated ROS, 60  $\mu$ M N-isobutyl-N-(4-methoxyphenylsulfonyl)glycyl hydroxamic acid (NNGH), 1 mM N-acetyl-L-cysteine (NAC) and 20  $\mu$ M EUK-8 were added to media during MMP-3 treatment. Thereafter, the ROS level was determined using fluorescence intensity. Panels (a) and (b) show the dose-dependent effect of MMP-3, and the effect of an MMP-3 inhibitor and antioxidant on ROS generation, respectively, in RAW264 cells, microphotographs shown in the panels being representative ones of at least three independent experiments. Panel (c) shows the effect of MMP-3 and NAC treatment on the cell viability determined by a 3[4,5-dimethyl-2-thiazolyl]-2,5-diphenyl-2H-tetrazolium bromide (MTT) assay. After cells were treated with 12.5 ng/mL recombinant MMP-3 in HBSS for 1 h, they were incubated in fresh Dulbecco's modified Eagle's medium for 4 h, and then MTT assays were performed. Each point represents the mean  $\pm$  SE ( $n = 4$ ). Scale bar is 50  $\mu$ m.

by Peters *et al.*<sup>(18)</sup> but not with those by Polomano *et al.*<sup>(11)</sup> for which paclitaxel caused heat hyperalgesia. This discrepancy might be due to the difference in paclitaxel doses between the reports of Peter *et al.* (36 mg/kg) and Polomano *et al.* (8 mg/kg). On the other hand, ATF3 immunoreactivity was observed in the neuronal nuclei of the lumbar DRG of paclitaxel-treated rats (Fig. 1c,d), being similar to the results previously reported by other groups.<sup>(18,24,25)</sup> Therefore, the immunohistochemical results taken together with the behavioral events demonstrated that we developed suitable model rats to analyze paclitaxel-induced neuropathic pain.

In microarray analysis on the DRGs of our model rats, it was found that paclitaxel induced up-regulation of inflammatory and/or immune response-related genes in the DRGs (indicated by asterisks in Table 1). Of these genes, we showed that expression of mRNAs for MMP-3 and CD163 significantly increased in paclitaxel-treated DRGs (Fig. 2a,b), and increased expression of active forms of MMP-3 was confirmed by Western blotting (Fig. 2c,d).

To identify which type of cell expresses MMP-3 in DRGs, we used anti-S100 and anti-Iba1 antibodies. A large-sized ganglion sensory neuron among the neurons in DRGs predominantly express S100, as well as the glial cells of Schwann and satellite cells.<sup>(28)</sup> Double immunofluorescent study clearly revealed that MMP-3-expressing cells were large-sized ganglion sensory neurons costained with anti-S100 antibody (Fig. 3), but not with anti-Iba1 antibody which is a marker for macrophage (Fig. 4). Furthermore, we confirmed colocalization of MMP-3 and NF200, a phosphorylated 200 kDa neurofilament subunit, in large neuronal cell bodies of the DRGs<sup>(30)</sup> (data not shown). These findings indicate that paclitaxel administration induces the expression

of the MMP-3 in the large ganglion neurons exclusively in the lumbar DRG. We are currently working in our laboratory on a project to elucidate the molecular mechanism underlying MMP-3 induction in paclitaxel-treated large ganglion neurons.

Recently, it has been reported *in vitro* that MMP-3 was secreted from cultured neurons under serum-free conditions or treatment with MPTP (1-methyl-4-phenylpyridinium).<sup>(26,31)</sup> Thus, it is considered that the up-regulated MMP-3 may be secreted by the large ganglion neurons of the paclitaxel-treated rat. We therefore tried to treat several types of neuronal cells, Neuro2a, SH-SY5Y, and PC12 with paclitaxel, but MMP-3 secretion into the media or up-regulation in the cells could not be detected in our experimental conditions (data not shown). To confirm MMP-3 secretion in the DRGs, further investigations are necessary, for example using primary cultured DRG neurons.

The up-regulation of MMP-3 occurred prior to accumulation of macrophages in the paclitaxel-treated DRGs (Fig. 4). This phenomenon clearly indicates that up-regulated MMP-3 in the large ganglion neurons proceeds to accumulate macrophages in the DRGs. Furthermore, we demonstrated that MMP-3 activated RAW264 macrophages (Fig. 5). Therefore, MMP-3 may be a critical molecule that induces the accumulation and activation of macrophages in the DRGs.

As described in the introduction, paclitaxel-induced peripheral neuropathy is generally known to be distributed in the 'glove and stocking' area and has been believed to disturb axoplasmic flow in peripheral nerves resulting from disorganization of microtubule functions.<sup>(5,8)</sup> In contrast, it has recently been reported that administration of paclitaxel could induce neuropathy without any morphological change.<sup>(11)</sup> In the case of our model, we did not observe an apparent morphological alteration in the

dorsal root (data not shown). Thus, we proposed a new hypothesis that the up-regulated MMP-3 induced by paclitaxel in large ganglion neurons accumulates and activates macrophages in the DRGs. This phenomenon may be one of the prior events enabling the development of peripheral neuropathy. To confirm our hypothesis, we have examined the pretreated effect of minocycline on a chain of events induced by paclitaxel. Minocycline is a MMP-3 inhibitor and has been reported to attenuate rat models of neuropathic pain.<sup>(32)</sup> Our preliminary result showed that minocycline inhibited up-regulation of MMP-3 and accumulation of macrophages at the protein level in the paclitaxel-treated DRGs (data not shown). However, since minocycline has been known as an inhibitor for not only MMP-3 but also macrophage activation,<sup>(32)</sup> we need more experiments to confirm our hypothesis against MMP-3–macrophage signaling on developing neuropathy.

Vincristin and cisplatin were also reported to induce neuropathy.<sup>(33,34)</sup> The mechanism to develop these neuropathies has a similar molecular basis to paclitaxel.<sup>(4)</sup> To clarify whether our hypothesis is applicable to other anticancer drugs, we performed preliminary study on expression of target molecules in DRGs treated with oxaliplatin. Administration of oxaliplatin to rats did not cause the up-regulation of MMP-3 and CD163 mRNAs in

DRGs (Nishida *et al.* unpublished observations), suggesting that molecular mechanisms contributing to the development of neuropathy by paclitaxel might be different to oxaliplatin. We need to analyze the mechanism in more detail to confirm our hypothesis.

In conclusion, we have developed a model of paclitaxel-induced neuropathy with representative symptoms, such as mechanical hyperalgesia and induction of the nerve injury marker ATF3 expression in the lumbar DRGs. Using this model, we have shown that MMP-3 expression is up-regulated in large ganglion neurons and that the accumulation of macrophages was induced in the DRGs. We further found that MMP-3 could activate macrophages *in vitro*. From these findings, we strongly suggest that up-regulation of MMP-3 is a significant event that triggers a series of reactions for the development of neuropathy and could be a target molecule to treat paclitaxel-induced neuropathic pain.

## Acknowledgment

Part of this work was supported by a Grant-in-Aid for General Scientific Research from the Ministry of Education, Culture, Sports, Science, and Technology of Japan (18590145).

## References

- Rowinsky EK. Update on the antitumor activity of paclitaxel in clinical trials. *Ann Pharmacother* 1994; **28**: S18–22.
- Socinski MA. Single-agent paclitaxel in the treatment of advanced non-small cell lung cancer. *Oncologist* 1999; **4**: 408–16.
- Derry WB, Wilson L, Jordan MA. Substoichiometric binding of taxol suppresses microtubule dynamics. *Biochemistry* 1995; **34**: 2203–11.
- Dougherty PM, Cata JP, Cordella JV, Burton A, Weng HR. Taxol-induced sensory disturbance is characterized by preferential impairment of myelinated fiber function in cancer patients. *Pain* 2004; **109**: 132–42.
- Forsyth PA, Balmaceda C, Peterson K, Seidman AD, Brasher P, DeAngelis LM. Prospective study of paclitaxel-induced peripheral neuropathy with quantitative sensory testing. *J Neurooncol* 1997; **35**: 47–53.
- Stubblefield MD, Vahdat LT, Balmaceda CM, Troxel AB, Hesdorffer CS, Gooch CL. Glutamine as a neuroprotective agent in high-dose paclitaxel-induced peripheral neuropathy: a clinical and electrophysiologic study. *Clin Oncol (R Coll Radiol)* 2005; **17**: 271–6.
- Bianchi G, Vitali G, Caraceni A *et al.* Symptomatic and neurophysiological responses of paclitaxel- or cisplatin-induced neuropathy to oral acetyl-L-carnitine. *Eur J Cancer* 2005; **41**: 1746–50.
- Rowinsky EK, Chaudhry V, Cornblath DR, Donehower RC. Neurotoxicity of Taxol. *J Natl Cancer Inst Monogr* 1993; **15**: 107–15.
- Theiss C, Meller K. Taxol impairs anterograde axonal transport of microinjected horseradish peroxidase in dorsal root ganglia neurons in vitro. *Cell Tissue Res* 2000; **299**: 213–24.
- Fazio R, Quattrini A, Bolognesi A *et al.* Docetaxel neuropathy: a distal axonopathy. *Acta Neuropathol* 1999; **98**: 651–3.
- Polomano RC, Mannes AJ, Clark US, Bennett GJ. A painful peripheral neuropathy in the rat produced by the chemotherapeutic drug, paclitaxel. *Pain* 2001; **94**: 293–304.
- Horie H, Takenaka T, Ito S, Kim SU. Taxol counteracts colchicine blockade of axonal transport in neurites of cultured dorsal root ganglion cells. *Brain Res* 1987; **420**: 144–6.
- Authier N, Gillet JP, Fialip J, Eschaler A, Coudore F. Description of a short-term Taxol-induced nociceptive neuropathy in rats. *Brain Res* 2000; **887**: 239–49.
- Matsumoto M, Inoue M, Hald A, Xie W, Ueda H. Inhibition of paclitaxel-induced A-fiber hypersensitization by gabapentin. *J Pharmacol Exp Ther* 2006; **318**: 735–40.
- Hudson LJ, Bevan S, Wotherspoon G, Gentry C, Fox A, Winter J. VR1 protein expression increases in undamaged DRG neurons after partial nerve injury. *Eur J Neurosci* 2001; **13**: 2105–14.
- Zhang X, Bao L, Shi TJ, Ju G, Elde R, Hökfelt T. Down-regulation of mu-opioid receptors in rat and monkey dorsal root ganglion neurons and spinal cord after peripheral axotomy. *Neuroscience* 1998; **82**: 223–40.
- Shi TS, Winzer-Serhan U, Leslie F, Hökfelt T. Distribution and regulation of alpha (2)-adrenoceptors in rat dorsal root ganglia. *Pain* 2000; **84**: 319–30.
- Peters CM, Jimenez-Andrade JM, Jonas BM *et al.* Intravenous paclitaxel administration in the rat induces a peripheral sensory neuropathy characterized by macrophage infiltration and injury to sensory neurons and their supporting cells. *Exp Neurol* 2007; **203**: 42–54.
- Zimmermann M. Ethical guidelines for investigations of experimental pain in conscious animals. *Pain* 1983; **16**: 109–10.
- Kozako T, Kawachi A, Cheng SB *et al.* Role of the vestibular nuclei in endothelin-1-induced barrel rotation in rats. *Eur J Pharmacol* 2002; **454**: 199–207.
- Matthiesen S, Lindemann D, Warnken M, Juergens UR, Racke K. Inhibition of NADPH oxidase by apocynin inhibits lipopolysaccharide (LPS) induced up-regulation of arginase in rat alveolar macrophages. *Eur J Pharmacol* 2008; **579**: 403–10.
- Lowry OH, Rosebrough NJ, Farr AL, Randall RJ. Protein measurement with the Folin phenol reagent. *J Biol Chem* 1951; **193**: 265–75.
- Tsujino H, Kondo E, Fukuoka T *et al.* Activating transcription factor 3 (ATF3) induction by axotomy in sensory and motoneurons: a novel neuronal marker of nerve injury. *Mol Cell Neurosci* 2000; **15**: 170–82.
- Jimenez-Andrade JM, Peters CM, Mejia NA, Ghilardi JR, Kuskowski MA, Mantyh PW. Sensory neurons and their supporting cells located in the trigeminal, thoracic and lumbar ganglia differentially express markers of injury following intravenous administration of paclitaxel in the rat. *Neurosci Lett* 2006; **405**: 62–7.
- Peters CM, Jimenez-Andrade JM, Kuskowski MA, Ghilardi JR, Mantyh PW. An evolving cellular pathology occurs in dorsal root ganglia, peripheral nerve and spinal cord following intravenous administration of paclitaxel in the rat. *Brain Res* 2007; **1168**: 46–59.
- Kim YS, Choi DH, Block ML *et al.* A pivotal role of matrix metalloproteinase-3 activity in dopaminergic neuronal degeneration via microglial activation. *FASEB J* 2007; **21**: 179–87.
- Suzuki K, Lees M, Newlands GF, Nagase H, Woolley DE. Activation of precursors for matrix metalloproteinases 1 (interstitial collagenase) and 3 (stromelysin) by rat mast-cell proteinases I and II. *Biochem J* 1995; **305**: 301–6.
- Vega JA, del Valle-Soto ME, Calzada B, Alvarez-Mendez JC. Immunohistochemical localization of S100 protein subunits (alpha and beta) in dorsal root ganglia of the rat. *Cell Mol Biol* 1991; **37**: 173–81.
- Imai Y, Ibata I, Ito D, Ohsawa K, Kohsaka S. A novel gene *ibal* in the major histocompatibility complex class III region encoding an EF hand protein expressed in a monocytic lineage. *Biochem Biophys Res Commun* 1996; **224**: 855–62.
- Lawson SN, Waddell PJ. Soma neurofilament immunoreactivity is related to cell size and fiber conduction velocity in rat primary sensory neurons. *J Physiol* 1991; **435**: 41–63.
- Kim YS, Kim SS, Cho JJ *et al.* Matrix metalloproteinase-3: a novel signaling proteinase from apoptotic neuronal cells that activates microglia. *J Neurosci* 2005; **25**: 3701–11.
- Mika J, Osikowicz M, Makuch W, Przewlocka B. Minocycline and pentoxifylline attenuate allodynia and hyperalgesia and potentiate the effects of morphine in rat and mouse models of neuropathic pain. *Eur J Pharmacol* 2007; **560**: 142–9.
- Sandler SG, Tobin W, Henderson ES. Vincristine-induced neuropathy. A clinical study of fifty leukemic patients. *Neurology* 1969; **19**: 367–74.
- Quasthoff S, Hartung HP. Chemotherapy-induced peripheral neuropathy. *J Neurol* 2002; **249**: 9–17.